Supporting Information

A effective "precursor-transformation" route toward high-yield synthesis of ZIF-8 tubes

Ziyi Liu, Aiping Wu, Haijing Yan, Danni Su, Chengxu Jin, Hao Guo, Lei Wang, Chungui Tian*

The content of ESI

The color of water solution (the $CuSO_4$ is added to mark a color) can not be seen in wet state, but can be obvious seen after drying (Inset of Fig. S11d).

Experimental Section

Chemicals

Zinc acetate, Ethylene glycol (EG), 2-methylimidazole (2-MeIM), cyclohexane, N,N-Dimethylformamide (DMF), alcohol, n-heptane, n-hexane, tetraethoxysilane (TEOS) were purchased from Tianjin Fuyu Fine Chemical Co., Ltd. Dibutyltin dilaurate (DBTDL), ethylacetate, hexadecane, acetone, choroform and hydroxyl-polydimethylsiloxane (PDMS) with average M.W.115,000 were purchased from Shanghai Aladdin Biochemical Techology Co., Ltd. Methanol and tetrahydrofuran was purchased from Shanghai Titan Scientific Co., Ltd. All reagents were used as received without further purification.

The preparation of Zn-EG Precursor

The Zn-EG (zinc glycerol) precursor was prepared by the reaction of EG with anhydrous zinc acetate according to our previous report[S1]. In detail, the 4.0 g of anhydrous zinc acetate was added to a 250 mL round-bottom flask contained 100 mL of EG. The solution was heated to 150 ^{o}C and maintained at this temperature for 1 h in a oil bath. After naturally cooling to room temperature, the white Zn-EG solid was separated by several cycles of centrifugation/washing with ethanol. The "wet" Zn-EG precursor was stored with no need of drying (the drying can result the convection partial of Zn-EG into ZnO) for further synthesis of ZIF-8.

The preparation of ZIF-8 tubes

In a typical synthesis, 0.5 g 2-MeIM was first dissolved in 30 mL DMF (Solution A). Then, 1.5 g Zn-EG precursor was added into another 30 mL of DMF and treated by ultrasonation/stirring for 50 min to form a homogeneous dispersion (Dispersion B). The Solution A was added into Dispersion B and further stirred for 10 min. Final dispersion was transferred to a Teflon vessel with volume of 80 mL. The vessel was sealed and heated at 120 °C for 12 h. After naturally cooling to room temperature, the solids were separated by centrifugation at 4000 rpm, and washed with anhydrous ethanol for 3 times. The final solid was dried at 60 ^{o}C for 12 h under vacuum condition. The reaction times were tuned as 5 min, 2 and 24 h to realize the formation

process.

The preparation of dodecahedral ZIF-8 (D-ZIF-8)

ZIF-8 nanocrystals were synthesized according to a procedure described in a previous report.[S2] 810 mg of $Zn(NO_3)_2 \bullet 6H_2O$ was added in 40 mL of methanol and stirred until completely dissolved (Solution A). At the same time, the 526 mg of 2-MeIM was dissolved in 40 mL of methanol (Solution B). Two solution was mixed and stirred for 1 h, and finally stand for 12 hours without stirring at room temperature. the white ZIF-8 solid was separated by several cycles of centrifugation/washing with ethanol.

Characterizations

The structure of ZIF-8 was analyzed by scanning electron microscopy (SEM: Hitachi S-4800) and transmission electron microscopy (TEM: JEM-2100). Carbon-coated copper grids were used as sample holders for TEM analysis. Before SEM observation, the samples were coated with gold in vacuum to increase the conductivity. X-ray diffraction (XRD) is acquired on a Rigaku D/max-2600/PC X-ray diffractometer (Cu-Kα radiation, λ=1.5406 Å) with accelerating voltage of 40 kV and current of 40 mA. X-ray photoelectron spectroscopy (XPS) measurements were performed on VG ESCALAB MK II using an Mg Ka (1253.6 eV) achromatic X-ray radiation. All binding energies were calibrated with reference to the C1s peak at 284.6 eV. TG analysis was carried out on SDT600 thermal analyzer under air atmosphere (flow rate: 100 mL min^{-1}). The temperature was increased from room temperature to 800 ^oC with the gradient rate of 10 ^oC min^{-1}. A PE Spectrum One B IR spectrometer was used to record the fourier transform infrared spectra (FT-IR) spectrometer of the samples in the region of 400-4000cm^{-1} with KBr pellets. The N_2 adsorption-desorption isotherm was conducted by using a Micromeritics Tristar II. Brunauer–Emmett–Teller (BET) method was used to calculate the specific surface area and the Density-Functional-Theory (DFT) model was used to calculate the pore size distribution. Before the test, the samples were degassed for 6 h at 150 °C in vacuum.

The loading of ZIF-8 at sponge

The ZIF-8 can be used as adsorber of organic reagent by loading ZIF-8 on sponge.[S3] To this, the pre-crosslinking PDMS solution was prepared by the dissolution of 1 wt% hydroxyl PDMS, 0.1 wt% TEOS and 0.02 wt% DBTDL in n-heptane. Then, a certain amount of ZIF-8 powder was added to form uniform ZIF-8/PDMS suspension under ultrasound. The clean melamine sponge (1x1x1cm ^{3}) was immersed in the suspension of ZIF-8/PDMS. The sponge coated with ZIF-8 (T-ZIF-8@sponge) was obtained by drying at 80 ^{o}C for several hours. By changing the amount of ZIF-8, T-ZIF-8@sponges with different loads can be obtained. The optimal loading is about 0.021g/cm^3. and the maximum loading can reach 0.1g/cm^3.

Absorption measurements of oil and organic solvents

Absorption measurement was performed according to the procedure reported by Li and co-works.[S4] The T-ZIF-8@sponge was used as adsorber of oil and organic solvents. In the process, the T-ZIF-8@sponge was immersed in different organic solvents or oils mixed with water at room temperature to achieve adsorption equilibrium. The samples are taken out from solvents after adsorption equilibrium. In order to prevent the absorbed solvents from evaporating, a rapid weight measurement is needed. The formulas for calculating absorbance are: Absorbance = (W_{all}-W_{empty})/W_{empty}*100%, W_{all} and W_{empty} are the weights of absorbing organic solvents and blank, respectively.

For regeneration of the materials, the adsorbed organic solvent have been evaporated and collected by heating under reduced pressure at 60 ^{o}C.

The analysis about the formation process of T-ZIF-8

Previous studies have shown that the hollow structure can be formed followed the oriented attachment (aggregation) and ostwald ripening process.[S5] The oriented attachment is a process based on the aggregation of small particles along the certain direction to reduce total surface area and the surface energy. Zhang et al have shown the synthesis of hierarchical nanotubes constructed from interlayer-expanded $MoSe_2$ nanosheets by a combination of oriented attachment and ostwald ripening effects.[S6]

By the combination of previous report and a series of our experiments, we can primarily ascribe the formation of tube-like ZIF-8 to a combination of oriented attachment and ostwald ripening effects. At the initial step, the Zn-EG is peeled in DMF to form the irregular plates. After adding the 2-methylimidazole, the plates can be convert to irregular ZIF-8 particles based on the quickly replaced reaction of 2-MIM and EG units. The irregular ZIF-8 particles have processed the high surface energy, so as to tent to the aggregation to decrease their surface energy. With the prolonging the reaction, the 1-D aggregation can be formed by the attachment of small particles along 1-D direction. The formation of tube-like structure should be ascribed to simultaneous ostwald ripening process.[S7]

Table.S1 The samples and corresponding reaction conditions

	Sample	Reactant 1	Reactant 2	Solvent	Reaction condition
1	Zn-EG Precursor	$Zn(AC)_2$	EG	EG	150 °C 1h
2	Zn-EG-DMF-50	Zn-EG precursor	No	DMF	Ultrasonation/stirring for 50 min
3	T-ZIF-8-5min	Zn-EG-DMF-50	2-MeIM	DMF	Reaction at room temperature for 5 min
4	T-ZIF-8-2	Zn-EG-DMF-50	2-MeIM	DMF	Reaction at 120 °C for 2 h
5	T-ZIF-8	Zn-EG-DMF-50	2-MeIM	DMF	Reaction at 120 °C for 12 h
6	T-ZIF-8-24	Zn-EG-DMF-50	2-MeIM	DMF	Reaction at 120 °C for 24 h

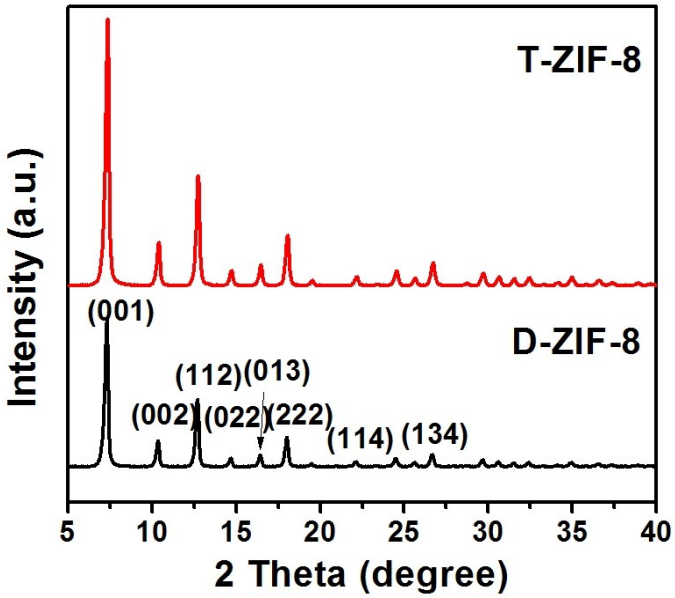

Fig. S1 XRD of T-ZIF-8 and D-ZIF-8.

Fig. S1 shows the XRD patterns of T-ZIF-8 and D-ZIF-8. We can see indential peak positions for two samples. The diffraction peaks at 2θ = 7.3°, 10.4°, 12.7°, 14.7°, 16.7°, 18.1° and 22.6° correspond to the (011), (002), (112), (022), (013), (222), (114), (134) plane of ZIF-8 crystals. The same XRD peaks of the samples indicate the formation of ZIF-8 by the reaction of Zn-EG and 2-MeIM.

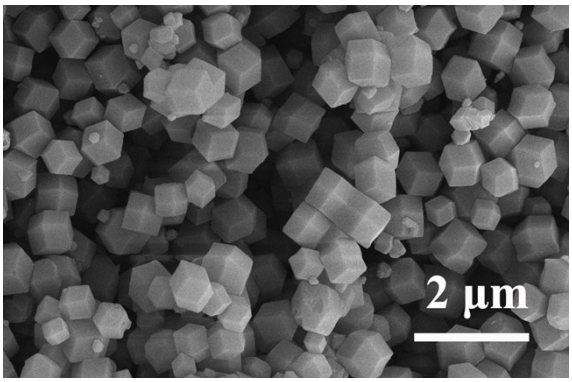

Fig.S2 SEM image of D-ZIF-8.

Fig.S2 shows TEM image of ZIF-8 synthesized by the reaction of $Zn(NO_3)_2$ with 2-MeIM in methanol. The samples are composed of polyhedrons with size about 500 nm.

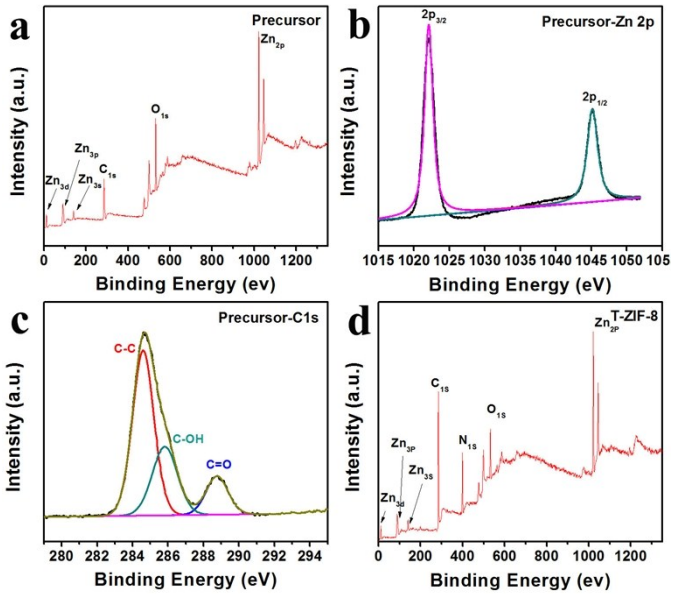

Fig.S3 (a) The survey spectrum of Zn-EG precursor, (b) Zn 2p spectrum of Zn-EG precursor, (c) C 1s spectrum of Zn-EG precursor and (d) the survey spectrum of T-ZIF-8.

The XPS spectrum of Zn-EG precursor shows the obvious C, Zn and O peaks. For spectra of Zn, the two peaks located at 1022.0 and 1044.9 eV can be assigned to Zn2p3/2 and Zn2p1/2. The C1s spectrum of Zn-EG can be fitted into three peaks centered at 284.6, 285.8 and 288.7 eV corresponding to C-C, C-OH and C=O in precursor. For T-ZIF-8, the wide XPS spectrum shows the presence of C, Zn and N peaks. The intensive peak of N implies the transformation of Zn-EG into ZIF-8.

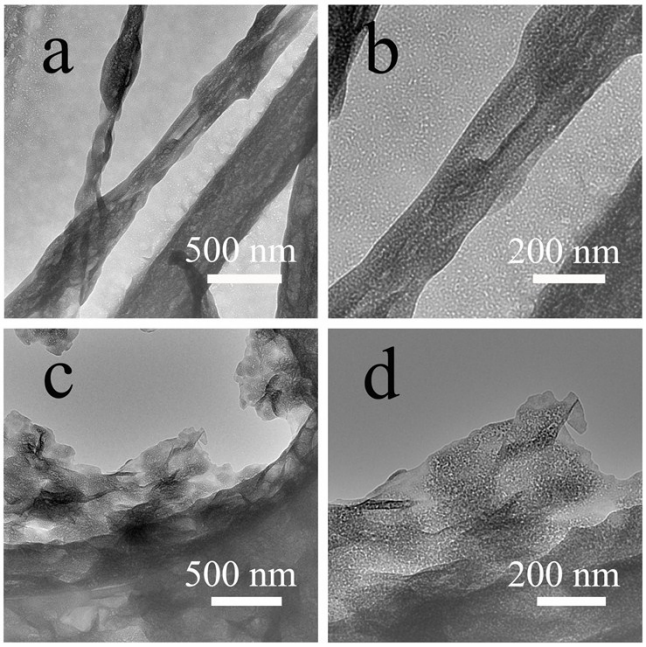

Fig.S4 The TEM images of the samples prepared by ultrasound treatment of Zn-EG precursor in DMF for (a,b) 10 min and (c,d) 50 min.

Fig.S4 shows the TEM images of the samples prepared by ultrasound treatment of Zn-EG precursor in DMF for 10 min (Zn-EG-DMF-10) (Fig. S4a and b) and 50 min (Zn-EG-DMF-50) (Fig. S4c and d). We can see the 1-D structure for Zn-EG-DMF-10, but with slight peeling on surface. For Zn-EG-DMF-50, the 1-D wire can not be observed, instead by many sheets. The results indicate that the precursor experiences the peeling process in DMF. The may be relative with the peeling effect in DMF, just like in the system of sulfide.[S8]

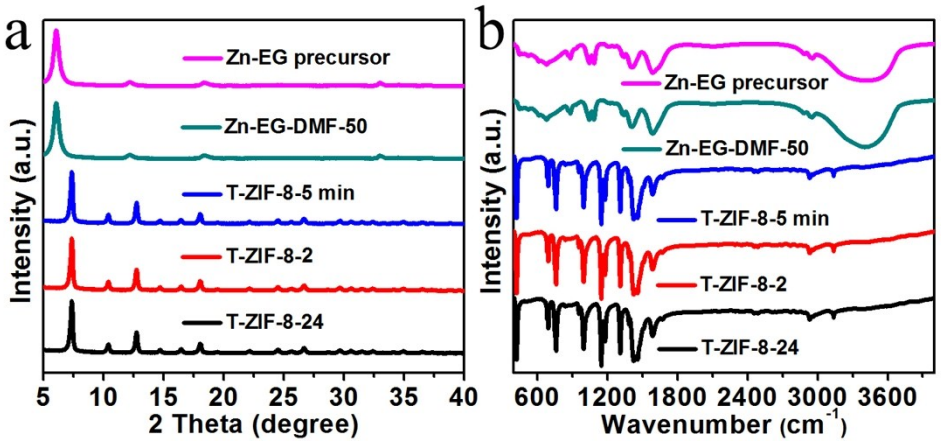

Fig.S5 (a) XRD patterns and (b) FT-IR spectra of different samples: Zn-EG precursor, Zn-EG-DMF-50, T-ZIF-8-5 min, T-ZIF-8-2 and T-ZIF-8-24.

Fig. S5 shows the XRD patterns and IR spectra of the samples from different treatment steps. The curve for Zn-EG precursor is also provided as comparison. The treatment in DMF for 50 min do not induce the obvious change of the precursor structure because of same XRD patterns of Zn-EG precursor and Zn-EG-DMF-50. After the reaction with 2-MeIM for 5min (T-ZIF-8-5min), 2h (T-ZIF-8-2) and 24 h (T-ZIF-8-24), we can observe the formation of ZIF-8. IR spectra have also show the results being consistent with that of XRD. Typically, there are same peaks for the Zn-EG precursor and Zn-EG-DMF-50. At the same time, the T-ZIF-8-5min, T-ZIF-8-2 and T-ZIF-8-24 show same IR spectra. The XRD and IR spectra indicate that the treatment in DMF do not change the structure of Zn-EG precursor. The ZIF-8 can be formed after adding the 2-MeIM in reaction system for short time.

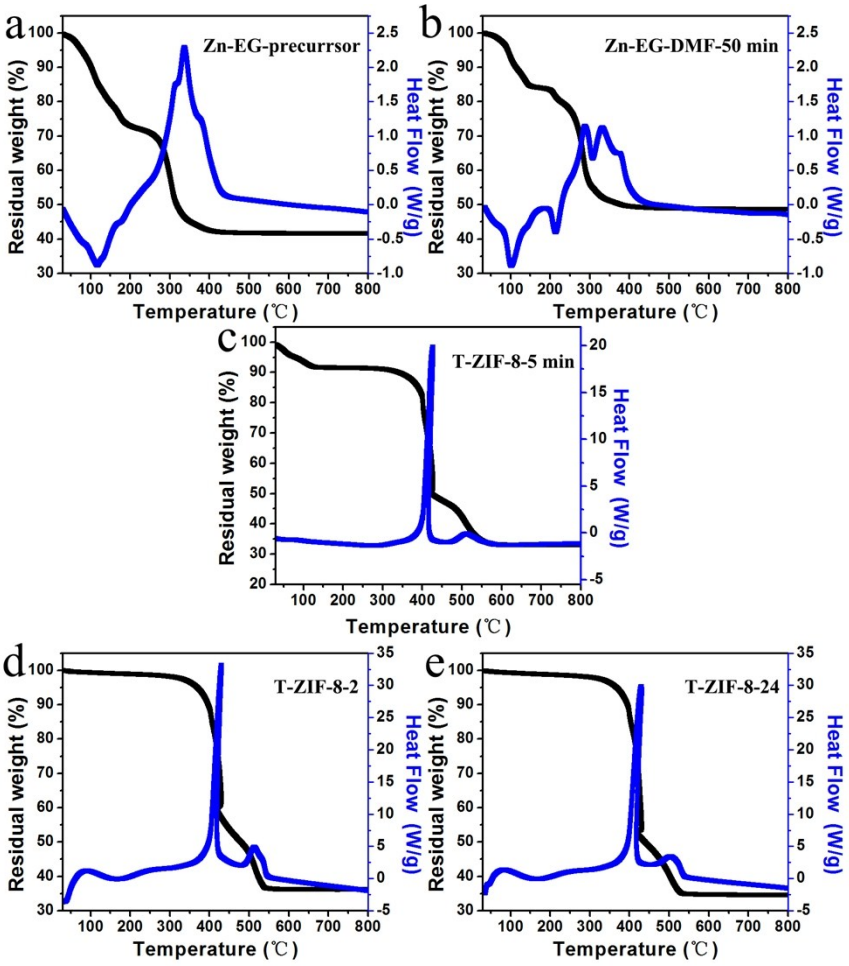

Fig.S6 TG curves of (a) Zn-EG precursor, (b) Zn-EG-DMF-50, (c) T-ZIF-8-5min, (d) T-ZIF-8-2 and (e) T-ZIF-8-24.

TG curves of Zn-EG precursor, Zn-EG-DMF-50, T-ZIF-8-5min, T-ZIF-8-2 and T-ZIF-8-24 samples in air are shown in Fig. S5. We can see the similar characteristics for Zn-EG precursor and Zn-EG-DMF-50 (Fig. S5 a and b), including the similar percentage (40-50%) and temperature (about 300^{o}C) of loss weight. After the reaction of Zn-EG-DMF-50 with 2-MeIM for 5 min, the TG curves show a obvious change. As show in Fig. S5c, the T-ZIF-8-5 min is stable at the temperature lower than 350 ^{o}C. There is obvious endothermic peak at about 400 ^{o}C. The loss weight is about 65% in the range of 350~550 ^{o}C. After 550 ^{o}C, there are no obvious loss weight. The characteristics are consistent with that of T-ZIF-8-2, T-ZIF-8-12 and T-ZIF-8-24 and D-ZIF-8. The results indicate the fast reaction of Zn-EG-DMF-50 with 2-MeIM to form ZIF-8.

Fig. S7 The photos of T-ZIF-8 samples from 3 times of parallel syntheses in 60 mL DMF.

Fig. S7 shows the photos of T-ZIF-8 samples from 3 times of parallel syntheses in 60 mL of DMF. The quality of the T-ZIF-8 is about 2.1 g. The yield is over 90% calculated on the Zn. The yield is much higher than those for D-ZIF-8 (about 20%)[S2], cubic ZIF-8 (about 45%) and ZIF-8 from modified dry-gel conversion methods (about 60%). The high yields should be favorable for their application.

The synthetic procedures for control ZIF-8 are as follows:

(1) **The Cubic ZIF-8 is synthesized according to the literature with slight modification[S9] as follows**: 0.29 g zinc nitrate hexahydrate was dissolved in 10 mL of deionized (DI) water (Solution A); Then, 4.54 g of 2-methylimidazole and 0.01wt% of CTAB were dissolved in 70 mL DI water (Solution B). Then, the solution A and B mixed them and stirred for 5 min at room temperature, and the resulting synthesis solution was transferred into Teflon-lined autoclaves for hydrothermal reaction at 120

^{o}C for 6 h. After that washing, sample collection. The yield is 0.0998g about 45% (based on the zinc salt index, the following data are same).

(2) **The dodecahedral ZIF-8 nanocrystals were prepared according to the previous report**[S2]: 810 mg of $Zn(NO_3)_2 \cdot 6H_2O$ in 40 mL of methanol stir until completely dissolved (Solution A) and 526 mg of 2-MeIM in 40 mL of methanol stir until completely dissolved (Solution B). After a mixing of two solutions, the mixture is vigorous stirred for 1 h and stand for 12 hours without stirring at room temperature. The white D-ZIF-8 solid was separated by several cycles of centrifugation/washing with ethanol. The mass of ZIF-8 is about 0.0805g, the yield is close to 20% based on the Zn.

(3) **The ZIF-8 was also synthesized by dry-gel conversion methods with slight modification**[S10]: 0.11 g (0.5 mmol) of zinc acetate dehydrate was mixed with 0.41 g (5 mmol) of MeIM. The mixture was placed in a 100 mL Teflon-lined stainless steel autoclave. H_2O (2.0 mL) was then added into the autoclave, and the autoclave was heated at 120 ^{o}C for 24 h. After the cooling and washing, the sample is collected. The mass of samples is about 0.0711g with a yields about 62%. The yield is similar to that in S10 (about 60%).

The proposed reason for the high yield of T-ZIF-8:

The "solid precursor" routes have been effective in the the synthesis of nano-structued materials.[S11] In the route, the desirable (main) elements are pre-incorporated in the precursor, and the final products are formed by the replacement reaction of foreign ions (ligand) with counter-charge ions in precursor. There are less loss of desirable elements in the synthesis, thus leading higher yields calculated on the basic of the elements. The Zn-EG precursor can be easily dispersed in DMF with relative high concentration. The high yield of T-ZIF-8 should be relative with using the pre-synthesized Zn-EG as solid precursor."

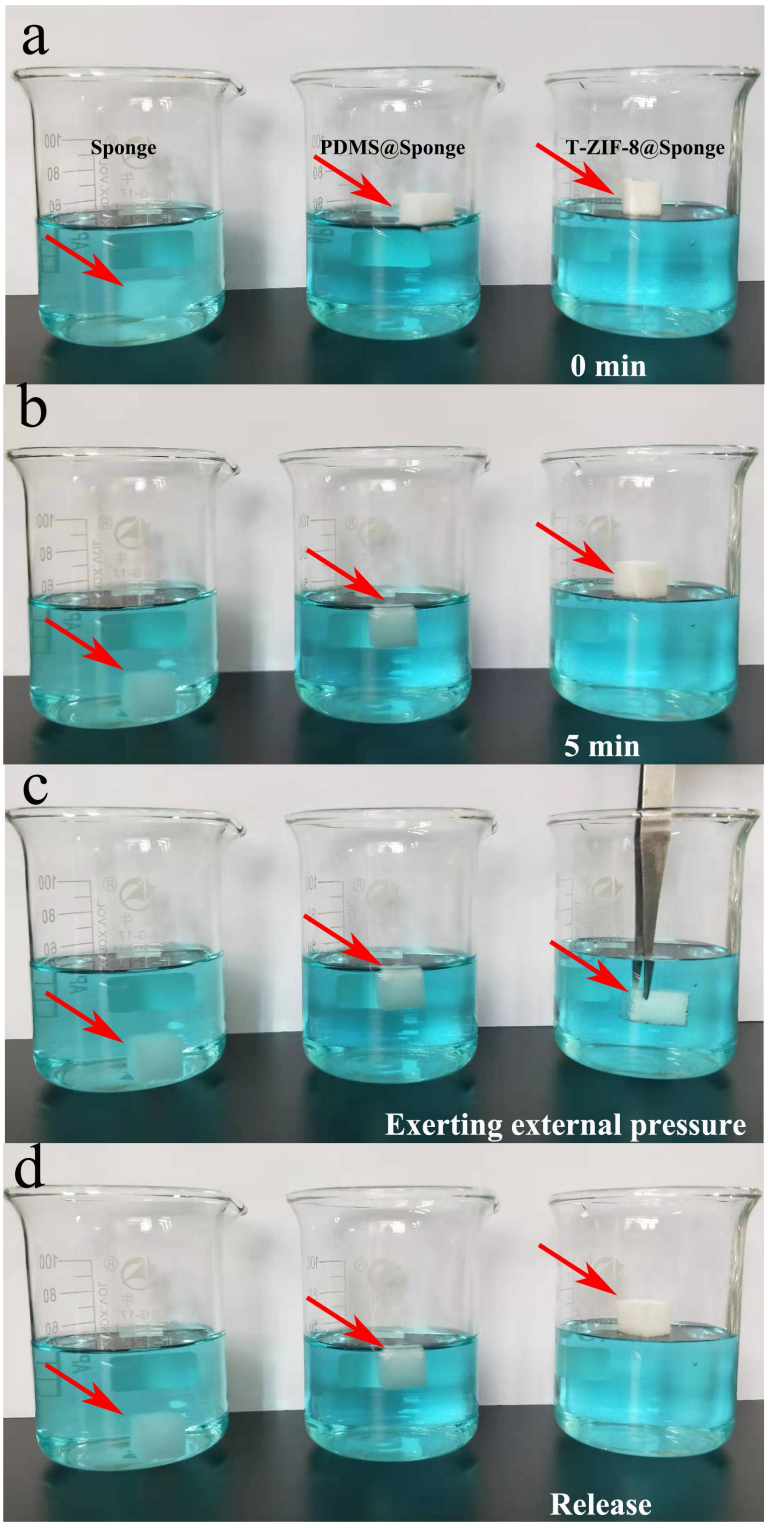

Fig. S8 The hydrophilic/hydrophobic ability test of sponge, sponge@PDMS, T-ZIF-8@sponge in water.

Figure S8 shows the photos about hydrophilic/hydrophobic ability of sponge (left), sponge@PDMS (middle) and T-ZIF-8@sponge. We can see the pure sponge

(left) sinks as soon as it enters the water. The results indicate the hydrophilic characteristics of sponge. In contrast, the sponge@PDMS (middle) and T-ZIF-8@sponge can stand on the water, indicating the hydrophobic characteristics of both samples. However, the sponge@PDMS sinks into water after placing for 5 min, while it is sill stand on the surface of water. In addition, a little pressure was used to impel the entry of T-ZIF-8@sponge in to the water. After remove the pressure, the T-ZIF-8@sponge float up again. The results indicate good hydrophobic ability of sponge modified by PDMS and ZIF-8 (T-ZIF-8@sponge).

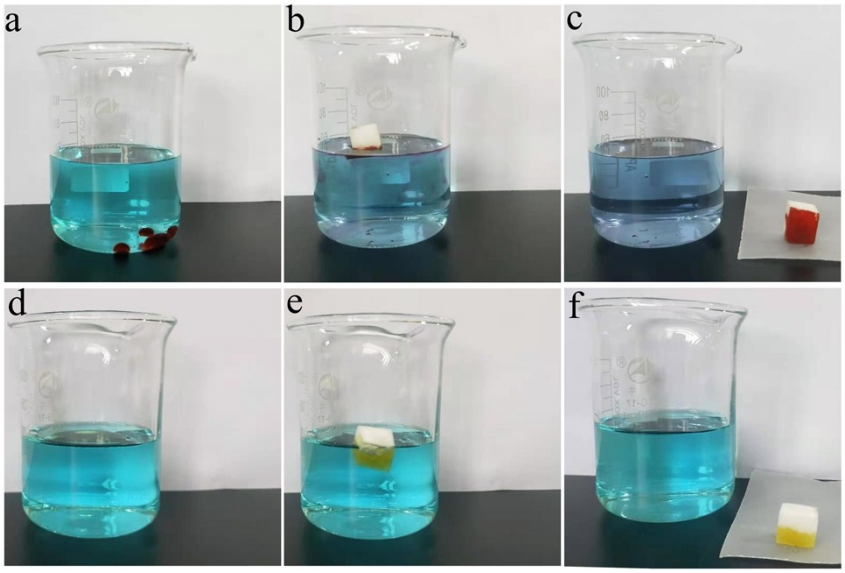

Fig. S9 Heavy oil (a,b,c) and light oil (d,e,f) absorbed by T-ZIF-8@sponge in the mixture of water and oil.

For the heavy oil, the T-ZIF-8@sponge is forced to contact chloroform in water. The heavy oil (methyl red dyed chloroform) sinking into the water instantly penetrates into the T-ZIF-8@sponge and are absorbed completely in a few seconds, thus giving a transparent area without pollution (clean water). In addition, the T-ZIF-8@sponge can absorbed the light oil on the surface of water rapidly through capillary force within few seconds and the clean water can be leaved.

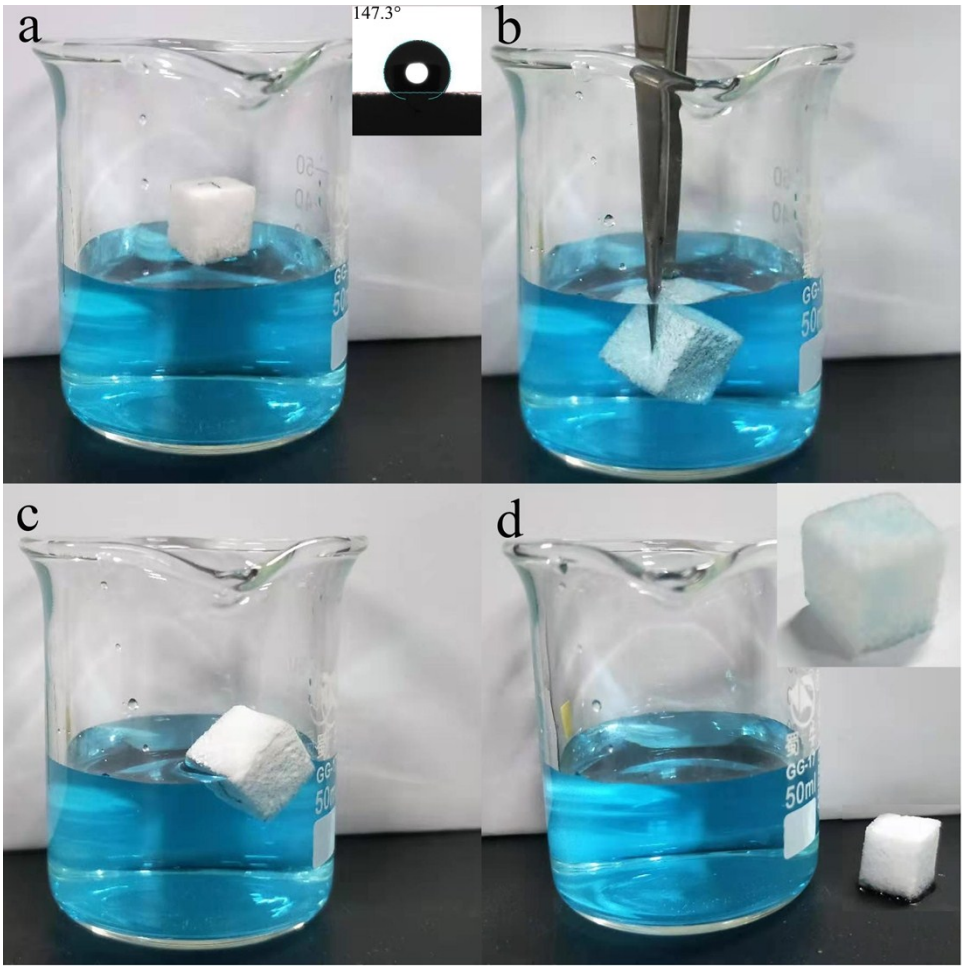

Fig. S10 The hydrophilic/hydrophobic ability test of D-ZIF-8@sponge.

Figure S10 shows the photos about hydrophilic/hydrophobic ability of D-ZIF-8@sponge. We can see the D-ZIF-8@sponge can stand on the water, indicating the hydrophobic characteristics. However, the hydrophobic angle is less than 150^{o}, which is lower than about 170^{o}C of T-ZIF-8@sponge. In addition, a little pressure was used to impel the entry of D-ZIF-8@sponge in to the water. After remove the pressure, the D-ZIF-8@sponge can float up the water, but with partial sink. After taking the D-ZIF-8@sponge from water, we can see some water on the materials. After drying, the blue color from water can be seen. The results indicated the hydrophobic property of the D-ZIF-8@sponge, but it is slight poor than that of T-ZIF-8@sponge.

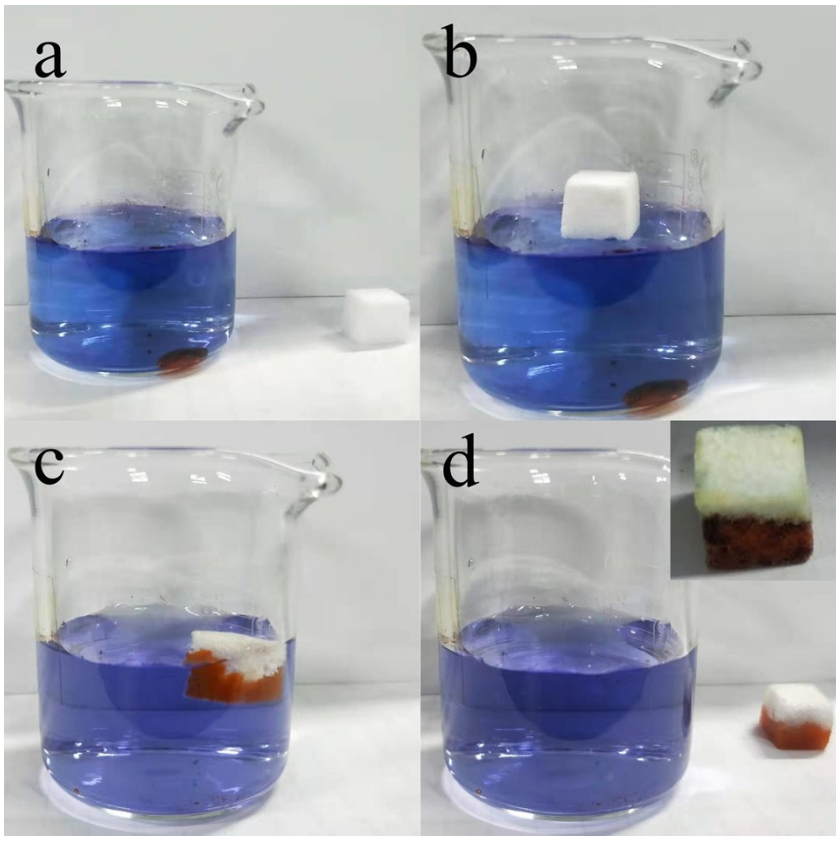

Fig. S11 Heavy oil absorbed by D-ZIF-8@sponge in the mixture of water and oil. The color of water solution (the $CuSO_4$ is added to mark a color) can not be seen in wet state, but can be obvious seen after drying (inset of Fig. S11d).

Figure S11 shows the performance of the D-ZIF-8@sponge for the separation of the heavy oil from water (Fig. S11 a-c). First, the D-ZIF-8@sponge is forced to contact chloroform in water. The heavy oil (methyl red dyed chloroform) in the water can be adsorbed into the D-ZIF-8@sponge in a few seconds. However, some water are also adsorbed into the D-ZIF-8@sponge (Fig. S11 d) that shows the blue color after drying. In addition, the relative weak hydrophilic ability makes the partial sink of D-ZIF-8@sponge in water, which is not favorable for the separation of light oils (it can float on water) from water.”**.**

Reference

(S1) C. G. Tian, W. Li, Q. Zhang, K. Pan, H. G. Fu, *Mater. Res. Bull.*, 2011, **46**, 1283–1289.

(S2) J. Tang, R. R. Salunkhe, J. Liu, N. L. Torad, M. Imura, S. Furukawa and Y. Yamauchi, *J. Am. Chem. Soc*., 2015, **137**, 1572−1580.

(S3) J. H. Gu, H. W. Fan, C. X. Li, J Caro and H Meng*, Angew. Chem. Int. Ed.*, 2019, **58**, 1–6.

(S4) A. Li, H. X. Sun, D. Z. Tan, W. J. Fan, S. H. Wen, X. J. Qing, G. X. Li, S. Y. Li, W. Q. Deng, *Energ. Environ. Sci.* 2011, **4**, 2062– 2065.

(S5): B. W. Li and H. C. Zeng, *Adv. Mater*. 2019, **31**, 1801104.

(S6):J. J. Zhang, M. H. Wu, T. Liu, W. P. Kang and J. Xu, *J. Mater. Chem. A,* 2017, **5,** 24859.

(S7) W. Z. Ostwald, *Phys. Chem*., 1900, **34**, 495.

(S8) J. N. Coleman, M. Lotya, A. O'Neill, S. D. Bergin, P. J. King, U. Khan, K. Young, A. Gaucher, S. De, R. J. Smith, I. V. Shvets, S. K. Arora, G. Stanton, H. Y. Kim, K. Lee, G. T. Kim, G. S. Duesberg, T. Hallam, J. J. Boland, J. J. Wang, J. F. Donegan, J. C. Grunlan, G. Moriarty, A. Shmeliov, R. J. Nicholls, J. M. Perkins, E. M. Grieveson, K. Theuwissen, D. W. McComb, P. D. Nellist, V. Nicolosi, *Science*, 2011,**331**, 568–571.

(S9) Y. C. Pan, D. D. Heryadi, F. Zhou, L. Zhao, G. Lestari, H. B. Su and Z. P. Lai, *CrystEngComm*, 2011, **13**, 6937 – 6940.

(S10) Q. Shi, Z. F. Chen, Z. W. Song, J. P. Li, and J. X. Dong*, Angew. Chem. Int. Ed.* 2011, **50**, 672 – 675.

(S11) Y. F. Yu, Y. M. Shi, and B. Zhang, *Acc. Chem. Res*. 2018, **51**, 1711−1721.